Macro- and Microdistributions of Boron Drug for Boron Neutron Capture Therapy in an Animal Model

YU-CHUAN LIN[1], JENG-JONG HWANG[2], SHYH-JEN WANG[3], BANG-HUNG YANG[3], CHI-WEI CHANG[4], MING-CHEN HSIAO[1] and FONG-IN CHOU[1,5]

[1]*Institute of Nuclear Engineering and Science, National Tsing Hua University, Hsinchu, Taiwan, R.O.C.;*
[2]*Department of Biomedical Imaging and Radiological Sciences, National Yang Ming University, Taipei, Taiwan, R.O.C.;*
[3]*Department of Nuclear Medicine and* [4]*National PET, Cyclotron Center, Taipei Veterans General Hospital, Taiwan, R.O.C.;*
[5]*Nuclear Science and Technology Development Center, National Tsing Hua University, Hsinchu, Taiwan, R.O.C.*

Abstract. *Background: The boron concentration (BC) in the blood, rather than in normal tissue, is often used as the reference to calculate the BC in tumor for boron neutron capture therapy (BNCT). The aims of this study were to justify whether BC in the blood is equal to that of normal tissue, and to verify the macro- and microdistributions of boron in tumor. Materials and Methods: BALB/c nude mice bearing SAS human oral carcinoma xenografts were intravenously injected with 400 mg/kg of boronophenylalanine (BPA). Macro- and microdistributions of boron in the tumor were assayed with ^{18}F-fluoro-L-boronophenylalanine-fructose (FBPA-Fr)/micro-positron-emission tomography (PET) and alpha track autoradiography, respectively. Results: The BCs assayed from the blood, normal tissue and tumor varied even on sampling at the same time points post-BPA administration. The ratio of BC in normal tissue to that in blood, i.e. N/B ratio, remains about 1.31 at 30 to 45 min post-BPA administration. Furthermore, ^{18}F-FBPA-Fr/micro-PET imaging and autoradiography also showed heterogeneous boron distribution in the tumor. Conclusion: The heterogeneous distribution of boron in the tumor is a limiting factor for the precise calculation of BC in the tumor. Here we suggest that the N/B ratio could be used to calculate the true BC in the tumor and in normal tissue for BNCT. ^{18}F-FBPA-Fr/PET imaging is useful to justify the N/B ratio for BNCT treatment.*

Correspondence to: Professor Fong-In Chou, Ph.D., Nuclear Science and Technology Development Center, National Tsing Hua University, No. 101, Section 2, Kuang-Fu Road, Hsinchu, Taiwan 30013, R.O.C., Tel: +886 35742884, Fax: +886 35725974, e-mail: fichou@mx.nthu.edu.tw

Key Words: Macrodistribution, microdistribution, heterogeneous distribution, boron drug, boron neutron capture therapy.

The success of boron neutron capture therapy (BNCT) is highly dependent on accurate calculation of the boron concentration (BC) in tumor and normal tissue and homogeneous distribution of boron in the tumor (1). Under BNCT treatment, the BC in blood is generally calculated as being equal to that in normal tissue and is used to calculate the BC in tumor. Thus, we examined the consistency of the BC between normal tissue and blood, and investigated boron microdistribution in the tumor region. BNCT is a binary treatment modality that depends on an optimal drug that contains ^{10}B and high-quality thermal neutrons. It is based on a nuclear reaction between the stable isotope (^{10}B) and a thermal neutron, and yields high linear energy transfer (LET) α and ^{7}Li particles. The path length of these heavy particles is in the range of 5-9 μm (around one cell diameter) in the tissue, and they have a high relative biological effectiveness (2, 3). Boronophenylalanine (BPA), an analog of tyrosine, has been utilized as a boron drug for BNCT, and accumulates in tumor more than in normal tissue. Neutron irradiation can begin at a suitable time when the BC in the tumor is sufficiently high and the tumor-to-normal tissue (T/N) ratio is effective. At a high T/N ratio, the tumor cells are destroyed with minimal damage to normal cells (4). Therefore, precisely calculating the macroscopic and microscopic distribution of boron can improve the therapeutic efficacy of BNCT.

^{18}F-BPA positron-emission tomography (PET) has been extensively utilized to determine the macrodistribution of boron drug and the T/N ratio before BNCT treatment (5, 6). In a clinical trial of BNCT, which included a clinical trial of BNCT for head and neck cancer at the Tsing Hua open pool reactor, the tumor to blood (T/B) ratio was assumed equal to T/N, to calibrate the boron dose in both tumor and normal tissue. The dose that could be tolerated by normal tissues that surround tumors was considered to be the limiting dose of radiation (7-9). However, the T/N ratio may not equal T/B;

boron drug in the blood is eliminated very rapidly and the BC in normal tissue gradually increases after BPA injection (10, 11). It has been reported that ratio of ^{18}F activity in tumor to that in normal brain (T/N) was not equal to that of the T/B after ^{18}F-BPA administration (5). The T/B ratio exceeded that of tumor to tongue ratio in a head and neck squamous cell carcinoma animal model after the intraperitoneal injection with BPA (12, 13). The pharmacokinetics of boron drug vary among tumor, blood and normal tissue. A conversion factor between T/B and T/N is required to accurately calculate the true BC in a tumor and normal tissue for BNCT. The normal tissue to blood (N/B) ratio and the microdistribution of boron drug in tumor in BNCT should therefore be evaluated.

Another important factor that determines the success of BNCT is the microdistribution of boron in a tumor. Neutron capture autoradiography (NCAR) using CR-39 nuclear track detectors has been applied to analyze the boron distribution in tumors. The track detector is easy to handle and sufficiently sensitive to α and ^{7}Li particles. It is very effective in NCAR (14-17). LR115 is a nuclear track detector, more efficient and sensitive for α-particles than is the CR-39 detector (18-20). In this study, the biodistribution of BPA and ^{18}F-FBPA-Fr/micro-PET images were used to evaluate the macrodistribution of boron drug, and an LR115 detector was used to investigate the microdistribution of boron in BALB/c nude mice bearing SAS cell xenografts.

Materials and Methods

Cell culture. A human oral squamous cell carcinoma cell line (SAS) was cultured in Dulbecco's modified essential medium (DMEM; GIBCO, Grand Island, NY, USA) that contained 10% heat-inactived fetal bovine serum (FBS), 100 U/ml penicillin and 100 μg/ml streptomycin (GIBCO) in a humidified atmosphere of 5% CO_2 and 95% air at 37˚C. A total of 2×10^6 cells were seeded in the T75 flask, and cells were harvested by trypsinization (0.05% trypsin).

Preparation of BPA-fructose solution. The BPA-fructose solution was prepared according a previous publication (21). Fructose (2.2 g) was dissolved in 30 ml double-deionized water to form the fructose solution. One gram of BPA (98% ^{10}B enrich; Syntagon, Sodertalje, Stockholm, Sweden) was added to the fructose solution and the pH value was adjusted to 9.5-10 using 5 N NaOH. The mixture was stirred until all of the powder had dissolved, and the pH value was readjusted to 7.4 using 1 N HCl. The BPA solution was filtered through a 0.2 μm filter, and the final BC of the BPA solution was 1200 ppm.

Animal model and BPA administration. Six-week-old male BALB/c nude mice were obtained from the National Laboratory Animal Center, ROC. Before the experiment, the mice were kept in a cage for at least one week at a temperature of 22±2˚C and a humidity of 50±10%. The animals had access to unlimited food and water. Mice were injected subcutaneously with 1×10^6 cells suspended in 100 μl phosphate buffered saline (PBS) into the forelimb under anesthesia with 2-3% isoflurane. When the tumor reached a suitable size (~70 mm^3), the mice were administered 400 mg/kg BPA *via* injection into a tail vein. Mice were sacrificed at 3, 15, 30, 45 and 60 min after BPA administration; the tumor, blood, mandible, tongue, heart, lung, liver, stomach, intestine, pancreas, spleen, and kidney were collected for BC analysis. The data were presented as the mean number of samples from 3 mice per treatment group that were analyzed individually.

BC analysis. Mouse tissue samples were stored at –20˚C. Each sample was thawed at room temperature and weighed in a Teflon tube. Three milliliters of 65% v/v nitric acid and 0.5 ml of hydrogen peroxide were added to the Teflon tube. The samples were digested in a microwave apparatus (MLS 1200 Milestone, Fatebenefratelli, Sorisole, Italy). The microwave digestion program was 3 min heating at 300 W, 2 min heating at 250 W, and cooling for 20 min. The resulting solution was diluted with double-deionized water to a total volume of 25 ml. BC analysis was performed by inductively coupled plasma-atomic emission spectroscopy (ICP-AES, OPTIMA 2000 DV; PerkinElmer Instruments, Norwalk, CT, USA). The analytical wavelength was 249.773 nm. The temperature of the argon plasma was 6000-7000 K, and the flow rate of the liquid was about 2 ml/min.

Preparation of ^{18}F-fluoro-L-boronophenylalanine fructose (^{18}F-FBPA-Fr). About 5.5 GBq ^{18}F-F_2 was produced from Ne that was mixed with 0.9% F_2 in an aluminum target body that was irradiated with 8.5 MeV deuteron for 2 hours at a beam current of 40 μA. [^{18}F]Acetyl hypofluorite was generated by passing ^{18}F-F_2 through a KOAc/AcOH column (flow rate, 50-60 ml/min). The [^{18}F]Acetyl hypofluorite was bubbled into 4 ml trifluoroacetic acid (TFA) that contained 20 mg BPA in a 5 ml Reacti-vial at ambient temperature. TFA was removed by N_2 gas (flow rate, 200 ml/min) under reduced pressure. The residue was dissolved in 2 ml acetic acid (0.1%), and then filtered through a 0.22 μm filter to yield the raw product. The raw product was purified using a reversed-phase semi-preparative high-performance liquid chromatography (HPLC) system. The ^{18}F-FBPA was eluted between 23 and 25 min and was collected. The solvent was removed under reduced pressure; sodium bicarbonate (0.5 ml, 8.4%) and fructose (1.0 ml, 0.5 mol/l) were then added and the solution was filtered through a 0.22 μm membrane filter into a sterile vial to yield the final product, ^{18}F-FBPA-Fr (22).

Dynamic micro-positron-emission tomographic (micro-PET) imaging and analysis. Dynamic micro-PET images of the SAS tumor-bearing mice were obtained using the micro-PET R4 system (Siemens, Knoxville, TN, USA). Each tumor-bearing mouse was anesthetized with 2-3% isoflurane and imaged in the prone position. The mouse was administered approximately about 7 MBq ^{18}F-FBPA-Fr (injected dose, ID) and immediately imaged. The dynamic image was acquired using 10 frames of 1 min, followed by 5 frames of 10 min for 60 min after ^{18}F-FBPA-Fr administration. The matrix size was 256×256 pixels. The field of view (FOV) was 7.89 cm, and the slice thickness was 0.423 mm. Regions of interest (ROIs) analysis used to quantify tumor tracer uptake were manually defined using the dedicated software AMIDE (23). The ^{18}F-FBPA-Fr distribution in the tumor was analyzed at –8.83, –10.52, and –14.33 mm from the centerline of the image (transverse plane). Adaptive isocontour threshold ROIs for the tumor were drawn on the transverse planes. The ROIs in the active

and non-active tumor regions were delineated to analyze ^{18}F-FBPA-Fr activity on the transverse planes at –9.68 to –11.37 mm from the centerline of the image. Active tumor regions were defined as those in which the mean activity exceeded 4 %ID/g. Non-active tumor regions were defined as those in which the maximum activity was below 2.7 %ID/g.

Autoradiographic analysis of microdistribution of boron in tumor. The mice were sacrificed and tumors were removed and frozen. Tumor sections with a thickness of 80 μm were prepared using a freezing microtome, and placed on a polymethyl methacrylate slide. LR115 films (Kodak-Pathe, Paris, France) were directly covered on the slide with a tumor section for neutron autoradiograpy. The slides were placed in a polyethylene (PE) phantom and irradiated with netrons for 20 min. The thermal neutron flux was 1.37×10^{10} n/cm^2/s at the exit of the beam. After neutron irradiation, the LR115 films were etched in 10% NaOH at a temperature of 58˚C for 10 min. The etched LR115 films were viewed under an optical microscope that was equipped with a digital camera to capture images of the α-tracks.

The intensity of the α-track images was 8 bits. The image resolution was 1600×1200 in RGB color mode, such that the highest image intensity did not exceed a pixel value of 256 in an individual channel. BC distributions were analyzed throughout the image and three profiles were obtained at y-positions of 600, 783, and 900 along the x-positions. The analyses yielded a relative BC distribution. The profile of intensity was processed using a program that was coded by Hsiao *et al*. (24, 25).

Statistical analysis. The data were expressed as mean±standard deviation (SD). Three mice per treatment group were analyzed individually. The difference of BC in tissues was analyzed by Student *t*-tests.

Results

Biodistribution of BPA in tumor-bearing mice. BCs of organs in tumor-bearing mice were analyzed at 15, 30, 45, and 60 min after the administering of a 400 mg/kg dose of BPA. The BCs of the mandible did not differ with time ($p>0.3$) after administration. Although the BC of skin and tongue began to decrease at 30 min, the BC of other normal tissue began to decrease 15 min after administration. The BC of tumor increased throughout the time-course of the experiment. However, the BC was mainly accumulated in the pancreas, and secondly in the kidney (Figure 1).

BCs and boron T/N and T/B ratios. The BCs of tumor at 3, 15, 30, 45 and 60 min after administration were 11.35±3.04, 15.77±3.71, 18.85±4.33, 19.7±5.06, and 19.97±5.45 ppm, respectively. The BC of tumor increased throughout the time-course of the experiment after BPA administration. The BCs of the tumor and muscle did not differ from each other ($p>0.3$) at either 3 or 15 min after administration (Figure 2A). The T/N ratios were 0.97 and 1.03 at 3 and 15 min after administration, respectively (Table I). The BC of muscle was used as the BC of normal tissue. The BC of muscle reached its maximum at 15 min, and then slowly decreased. The T/B ratio thus increased with time. The N/B ratio was stable between 30 and 45 min after administration at approximately 1.31 (Table I).

Table I. *The T/N, T/B and N/B boron concentration ratios in mice administrated boronophenylalanine (BPA).*

Ratio	Time (min) after administration				
	3	15	30	45	60
T/N	0.97	1.03	1.25	1.38	1.59
T/B	0.18	1.17	1.63	1.81	2.43
N/B	0.19	1.13	1.31	1.32	1.52

T: Tumor; N: normal tissue (muscle); B: blood; BPA dose: 400 mg/kg bw.

Distribution of ^{18}F-FBPA-Fr in tumor. Figure 3 shows the ^{18}F-FBPA-Fr distribution on the coronal plane of a mouse and three transverse planes in the tumor. Hot spots and cold spots were observed on the coronal planes of the tumor (Figure 3A). The three transverse planes of the tumor were –14.33 (plane 1), –10.52 (plane 2) and –8.83 mm (plane 3) from the centerline (transverse plane) of the image, respectively. Plane 1 was close to the tumor periphery and a region of high activity was observed at the center of the tumor (Figure 3B). On transverse plane 2, a large active region (R1) was observed on the left side of tumor and a region of low activity (R2) was also present in the tumor center (Figure 3C). The tumor activity of transverse plane 3 was apparently less than that on transverse planes 1 and 2, and a region with low activity was observed on the left side of the tumor (Figure 3D). The results provide evidence that a heterogeneous distribution of ^{18}F-FBPA-Fr existed in the tumor.

Table II shows tumor activity on different transverse planes after ^{18}F-FBPA-Fr administration. Planes 1, 2, 3, 4 and 5 were –9.68, –10.1, –10.52, –10.94 and –11.37 mm from the center distance of the transverse plane, respectively. The activity of ROI of the active tumor region and the non-active tumor region on each plane was analyzed. The ^{18}F-FBPA-Fr activity analysis provided evidence of heterogeneous distribution of activity of the active and non-active regions in the tumor.

Distribution of boron-10 in tumor. Figure 4A shows the section of a tumor located under the skin. A scar close to the skin was observed on the frozen section of the tumor and histomorphologic heterogeneity was observed in regions a, b and c of the tumor section. The autoradiograph displays the α-tracks on the same section of the tumor (Figure 4B). The track density was lower in region a, and tumor necrosis was

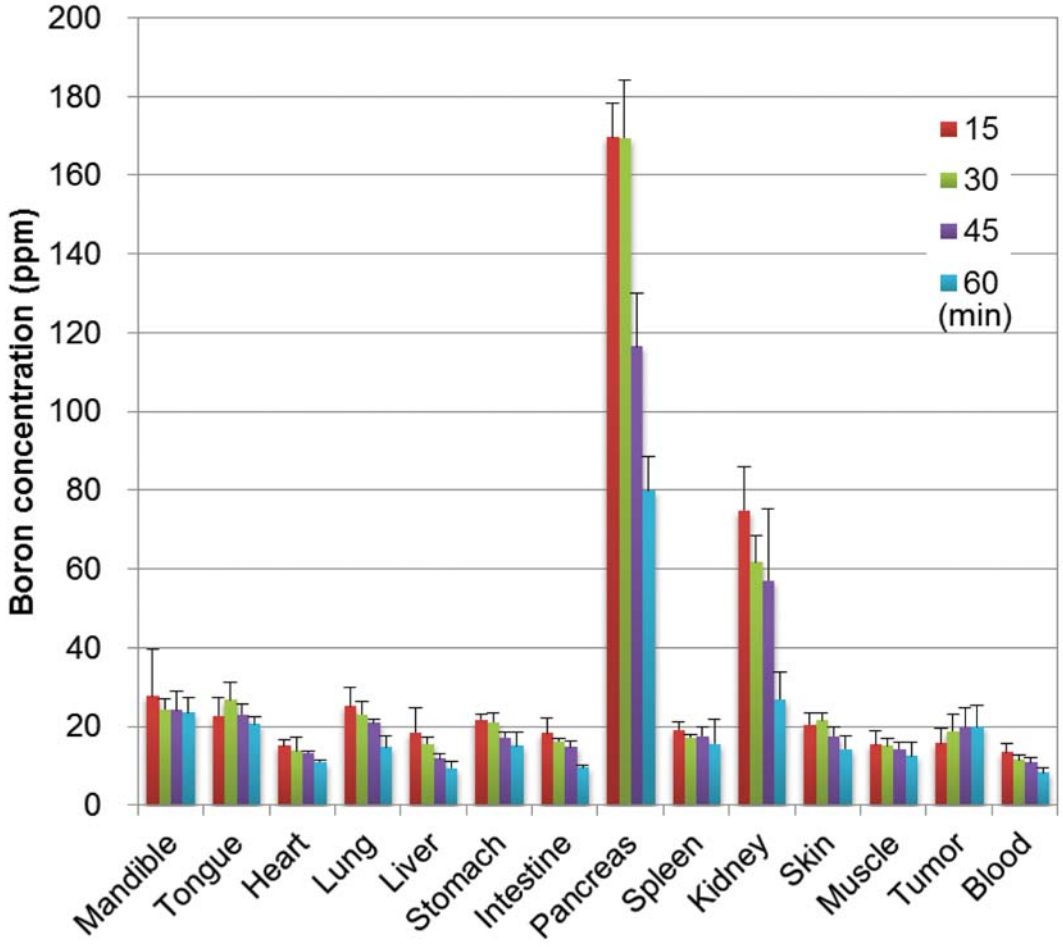

Figure 1. *Boron concentrations in organs of tumor-bearing mice after administration of 400 mg/kg/bw dose of boronophenylalanine (BPA). The data was presented as the mean number of samples from 3 mice per treatment group.*

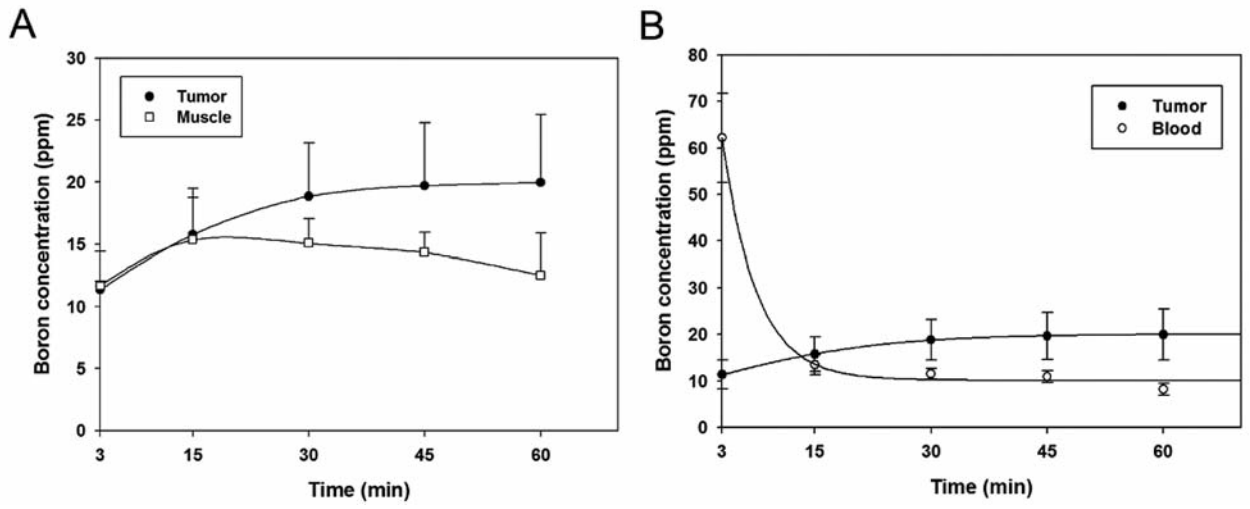

Figure 2. *Boron concentrations in tumor, muscle and blood at 3, 15, 30, 45 and 60 min after administration of a 400 mg/kg/bw dose of BPA. A: Boron concentrations in tumor and muscle; B: boron concentrations in tumor and blood. The data was presented as the mean number of samples from 3 mice per treatment group.*

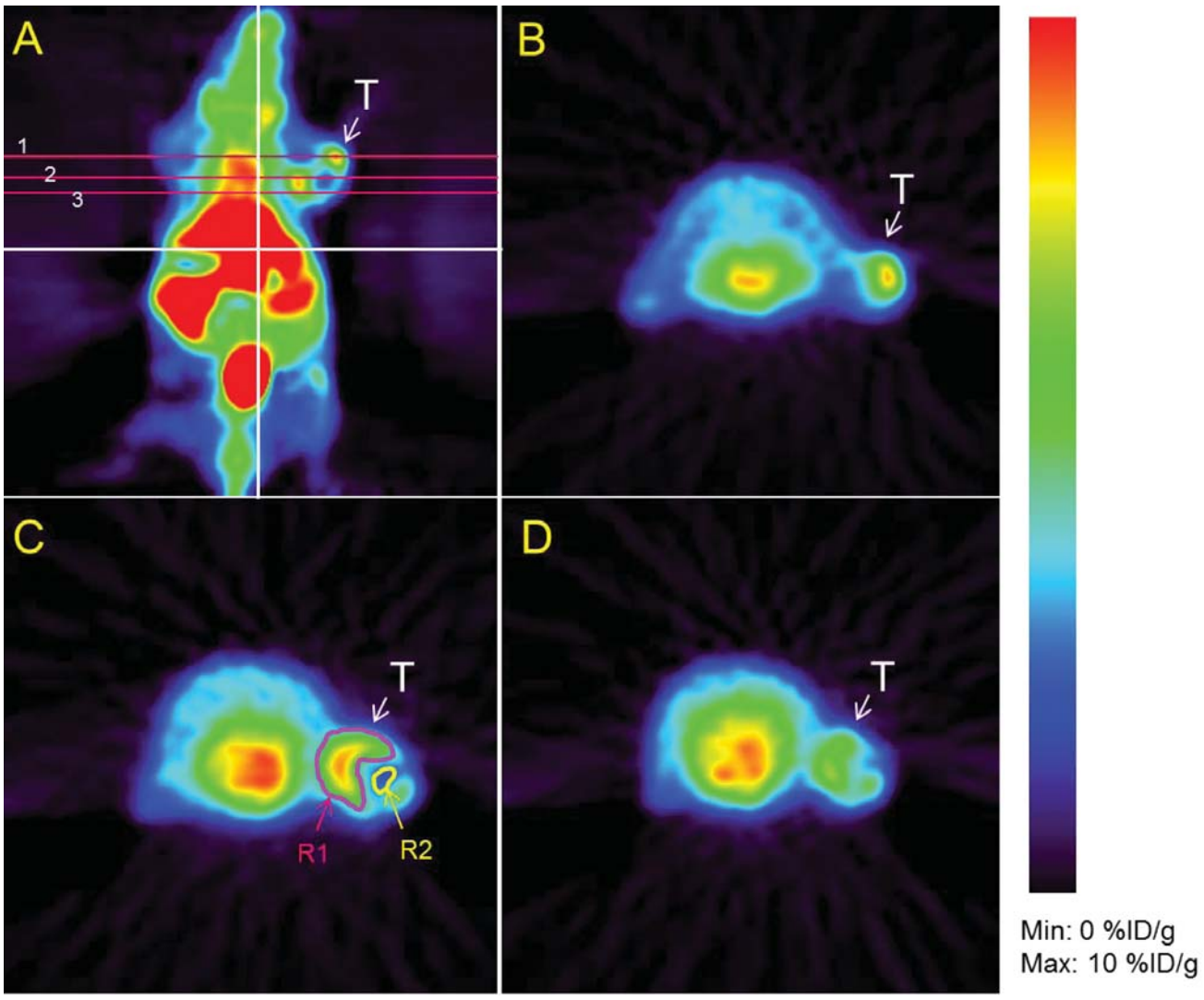

Figure 3. *A: Coronal view of micro-PET image in a mouse. B: Transverse plane 1; C: transverse plane 2; and D: transverse plane 3 at –14.33, –10.52 and –8.83 mm from the center of the image, respectively. The relative intensity of image reveals the relative ^{18}F-FBPA-Fr activity in tumor. T: Tumor, R1: active region in the tumor, R2: non-active region in the tumor.*

also observed in the same region, as presented in Figure 4A. The track density was higher in regions b and c, indicating active uptake of the boron drug by tumor cells in these regions. Figure 4C shows the relative intensity profile that corresponds to Figure 4B. In Figure 4C, regions of higher intensity and lower intensity can be seen. However, although in the region of higher intensity, the track density was not homogeneous. Figure 4D shows the profiles of the relative boron distribution at y-distance of 600, 783 and 900 along the x-positions on the tumor section in Figure 4C. The variation of relative α-track intensity was observed; the results provide evidence of the heterogeneous distribution of boron in the tumor.

Discussion

Before BPA-mediated BNCT treatment, the T/N ratio was determined by analyses of the ROI using ^{18}F-BPA PET (5, 26, 27). In BNCT treatment, the delivered radiation dose is limited by the tolerance of the surrounding normal tissues, in order to prevent normal tissues from damage (3). Because blood is easily obtained during BNCT treatment, the BC in blood is assumed to be equal to that in normal tissue in the calculation of the boron dose in both normal tissue and tumor (7, 28, 29). However, the T/B ratio has been reported not to equal T/N at 1, 2 and 3 hours after the intraperitoneal administration of BPA in a human oral cancer model (12). Moreover, Kreimann *et al*. investigated the biodistribution in

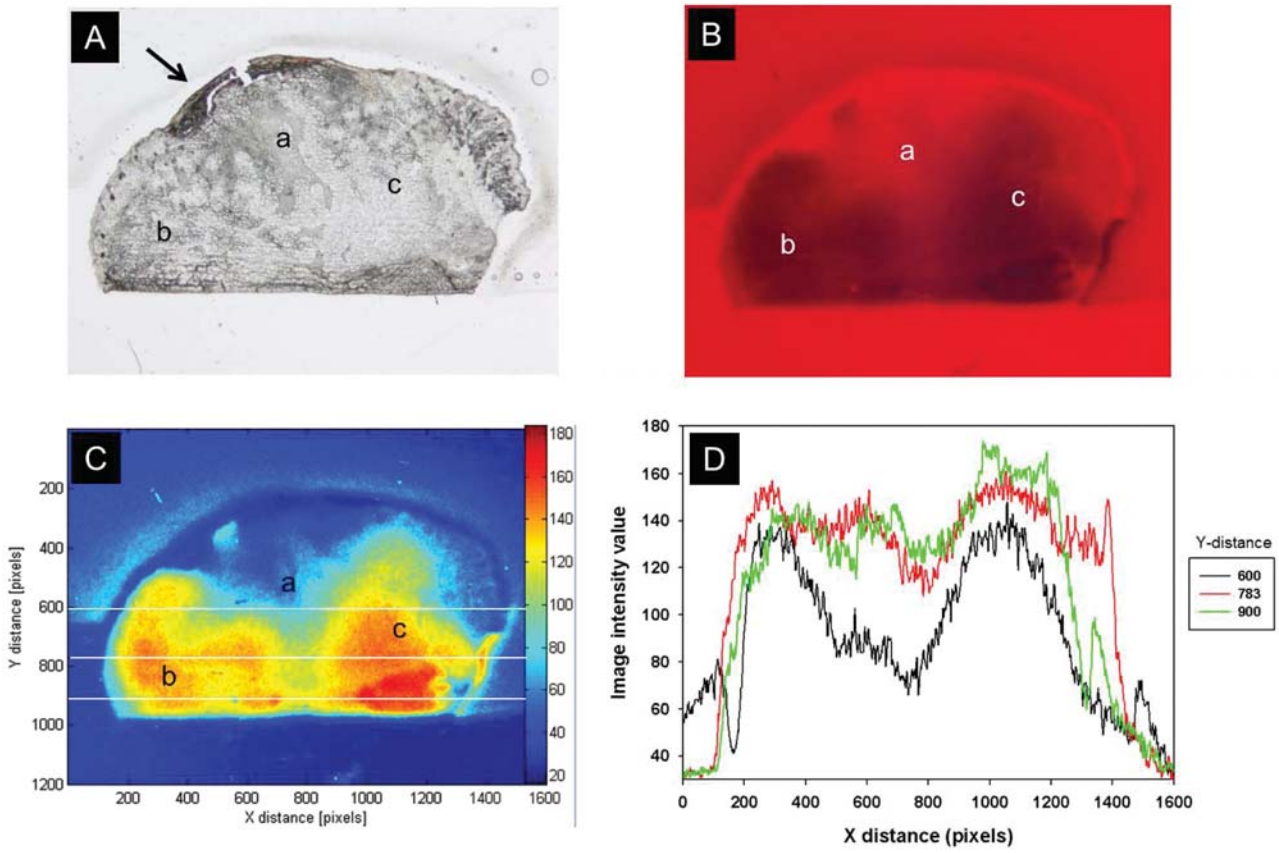

Figure 4. *Frozen section and autoradiograph of tumor after administration of a 400 mg/kg/bw dose of boronophenylalanine (BPA). A: 80 μm-thick frozen section of tumor; B: autoradiograph of tumor section; C: α-track intensity distribution in tumor autoradiograph; D: relative intensity profile of α-track at y-distances of 600, 783 and 900 along the x-positions on the tumor section. The size of tumor was 92.63 mm3. Arrow: Scar.*

a hamster cheek pouch model of oral cancer after intraperitoneal administration of a 300 mg/kg dose of BPA, and T/N ratios were not equal to T/B ratios at 0.5, 1, 1.5, 2.5, 3.5, 6 and 12 hours after BPA administration (13). In our study, at 3, 15, 30, 45 and 60 min after intravenous administration of a 400 mg/kg dose of BPA, the T/N ratio did not equal T/B at any time following BPA administration, and variations in T/B and T/N ratios related to the time of measurement were observed.

Boron doses that contributed most significantly to the effective dose for the tumor and normal tissue in BNCT treatment were calculated in real time. The estimate of the BC in tumor was based on the BC in blood, but the BC in the blood was not equal to that in normal tissue. Data of this study showed the BCs in blood were less than those in normal tissue. Using the blood BC as the basis for estimating tumor BC, tumor BCs were overestimated by 13.6%, 30%, 31% and 52.8%, respectively, at 15, 30, 45 and 60 min after BPA administration. However, normal tissue BCs were underestimated by 12%, 23.3%, 23.7% and 34.6%, respectively, at 15, 30, 45 and 60 min after BPA administration. Therefore, a conversion factor needs to be applied for estimating the true BC in tumor and normal tissue for the dose calculation during BNCT treatment. The conversion factor should be the N/B ratio. In our studies, N/B ratios were constant (~1.31) at 30 and 45 min after administration of a 400 mg/kg dose of BPA in a human oral squamous cell carcinoma-bearing animal model. The constancy of the N/B ratio facilitated the estimation of BC and boron dose calculation for the tumor and the maximum tolerated dose of normal tissue in BNCT. Thus, the T/N, T/B and N/B ratios should be determined by ROI analysis using ^{18}F-FBPA-Fr PET before a patient undergoes BNCT treatment.

The estimation of the BNCT dose assumes that the boron drug is homogeneously distributed in the tumor and in normal tissue (30). In fact, the homogeneity of BPA in the tumor depends on the tumor size and characteristics. The distribution of boron was more homogenous in small tumors than in larger tumors. It was evident that BPA was targeted

Table II. *^{18}F-FBPA-Fr activity in region of interest (ROI) of active and non-active tumor regions on transverse planes of mouse tumor.*

ROI	Plane no.	Volume (mm^3)	Min (%ID/g)	Max (%ID/g)	Mean (%ID/g)	Percentage error	
						Min activity (%)	Max activity (%)
Active tumor region	1	16.26	2.83	6.62	4.75	–40.38	39.3
	2	10.18	2.34	6.62	4.46	–47.44	48.29
	3	8.44	2.84	6.3	4.81	–40.88	31.15
	4	18.85	2.54	6.3	4.67	–45.69	34.98
	5	10.16	2.26	6.3	4.55	–50.34	38.56
Non-active tumor region	1	2	1.93	2.67	2.83	–8.87	26.3
	2	0.96	1.93	2.44	2.34	–8.52	15.72
	3	1.16	1.8	2.56	2.84	–13.44	23.52
	4	2.54	1.8	2.56	2.54	–13.73	23.11
	5	1.23	1.8	2.5	2.26	–13.06	21.04

Planes 1, 2, 3, 4 and 5 were at –9.68, –10.1, –10.52, –10.94 and –11.37 mm from the centerline of the image, respectively. Percentage error of minimum (min) activity (%)=(Min – mean)/mean×100%; percentage error of maximum (max) activity (%)=(Max – mean)/mean×100%. %ID/g: percentage injected dose per gram of tissue.

to actively dividing cells by the double labeling of mice with L-BPA and tritiated thymidine (31). Moreover, some of the tumor cells were at rest. These quiescent cells were arrested in the G_0 phase. The BC was lower in quiescent cells than in cells in other phases of the cell cycle after BPA treatment (32). BPA accumulation was higher in mouse squamous cell carcinoma (SCCVII) and rat glioma (C6) cells in the G_2/M than in those in the G_0/G_1 phase (33), which may possibly cause the heterogeneous distribution of boron drug.

^{18}F-FBPA-Fr activity was analyzed on five transverse sections of tumor. The minimum and maximum activities in the ROI on five transverse planes from –9.68 to –11.37 mm from the center of the image were greater in the active region of the tumor than in the inactive region (Table II). These results provide evidence that tumor cells in the same transverse section contained different concentrations of boron drug, and there may also be a low concentration of BPA in the active regions of the tumor. The percentage errors of minimum activity ranged from –40.38 to –50.43%, and these of maximum activity ranged from 31.15 to 48.29%. These results demonstrate the possible presence of various histological types and microdistributions of boron drugs within the tumor. The success of BNCT depends on an accurate calculation of the macro- and microdistributions of boron drug.

Acknowledgements

The Authors would like to thank the National Science Council of the Republic of China and the Veterans General Hospitals and University system of Taiwan for financially supporting this research under contracts no. NSC 98-2314-B-007-001-MY2, NSC 99-3111-B-007-001 and VGHUST101-G1-2-2, respectively. Micro-PET was supported by the Molecular and Genetic Imaging Core/National Research Program for Genomic Medicine at National Yang-Ming University. Ted Knoy is appreciated for his editorial assistance.

References

1 Coderre JA and Morris GM: The radiation biology of boron neutron capture therapy. Radiat Res *151*: 1-18, 1999.

2 Barth RF, Soloway AH, Fairchild RG and Brugger RM: Boron neutron capturetherapy for cancer. Realities and prospects. Cancer *70*: 2995-3007, 1992.

3 Smith DR, Chandra S, Coderre JA and Morrison GH: Ion microscopy imaging of 10_B from p-boronophenylalanine in a brain tumor model for boron neutron capture therapy. Cancer Res *56*: 4302-4306, 1996.

4 Lin YC, Wang SJ, Chung HP, Liu HM and Chou FI: Low dose of gamma irradiation enhanced boronophenylalanine uptake in head and neck carcinoma cells for boron neutron capture therapy. Appl Radiat Isot *69*: 1728-1731, 2011.

5 Kabalka GW, Smith GT, Dyke JP, Reid WS, Longford CP, Roberts TG, Reddy NK, Buonocore E and Hubner KF: Evaluation of fluorine-18-BPA-fructose for boron neutron capture treatment planning. J Nucl Med *38*: 1762-1767, 1997.

6 Aihara T, Hiratsuka J, Morita N, Uno M, Sakurai Y, Maruhashi A, Ono K and Harada T: First clinical case of boron neutron capture therapy for head and neck malignancies using ^{18}F-BPA PET. Head Neck *28*: 850-855, 2006.

7 Palmer MR, Goorley JT, Kiger WS, Busse PM, Riley KJ, Harling OK and Zamenhof RG: Treatment planning and dosimetry for the Harvard-MIT Phase I clinical trial of cranial neutron capture therapy. Int J Radiat Oncol *53*: 1361-1379, 2002.

8 Yu HT, Hsueh Liu YW, Lin TY and Wang LW: BNCT treatment planning of recurrent head-and-neck cancer using THORplan. Appl Radiat Isot *69*: 1907-1910, 2011.

9 Wang LW, Wang SJ, Chu PY, Ho CY, Jiang SH, Hsueh Liu YW, Liu YH, Liu HM, Peir JJ, Chou FI, Yen SH, Lee YL, Chang CW, Liu CS, Chen YW and Ono K: BNCT for locally recurrent head and neck cancer: Preliminary clinical experience from a phase I/II trial at Tsing Hua Open-Pool Reactor. Appl Radiat Isot *69*: 1803-1806, 2011.

10 Kiger WS, Palmer MR, Riley KJ, Zamenhof RG and Busse PM: A pharmacokinetic model for the concentration of ^{10}B in blood after boronophenylalanine-fructose administration in humans. Radiat Res *155*: 611-618, 2001.

11 Imahori Y, Ueda S, Ohmori Y, Sakae K, Kusuki T, Kobayashi T, Takagaki M, Ono K, Ido T and Fujii R: Positron emission tomography-based boron neutron capture therapy using boronophenylalanine for high-grade gliomas: Part II. Clin Cancer Res *4*: 1833-1841, 1998.

12 Obayashi S, Kato I, Ono K, Masunaga S, Suzuki M, Nagata K, Sakurai Y and Yura Y: Delivery of (10)boron to oral squamous cell carcinoma using boronophenylalanine and borocaptate sodium for boron neutron capture therapy. Oral Oncol *40*: 474-482, 2004.

13 Kreimann EL, Itoiz ME, Dagrosa A, Garavaglia R, Farias S, Batistoni D and Schwint AE: The hamster cheek pouch as a model of oral cancer for boron neutron capture therapy studies: selective delivery of boron by boronophenylalanine. Cancer Res *61*: 8775-8781, 2001.

14 Pazirandeh A, Jameie B and Zargar M: Determination of boron distribution in rat's brain, kidney and liver. Appl Radiat Isot *67*: S369-S373, 2009.

15 Mikado S, Yanagie H, Yasuda N, Higashi S, Ikushima I, Mizumachi R, Murata Y, Morishita Y, Nishimura R, Shinohara A, Ogura K, Sugiyama H, Iikura H, Ando H, Ishimoto M, Takamoto S, Eriguchi M, Takahashi H and Kimura M: Application of neutron capture autoradiography to boron delivery seeking techniques for selective accumulation of boron compounds to tumor with intra-arterial administration of boron entrapped water-in-oil-in-water emulsion. Nucl Instrum Meth A *605*: 171-174, 2009.

16 Altieri S, Bortolussi S, Bruschi P, Chiari P, Fossati F, Stella S, Prati U, Roveda L, Zonta A, Ferrari C, Clerici A, Nano R and Pinelli T: Neutron autoradiography imaging of selective boron uptake in human metastatic tumours. Appl Radiat Isot *66*: 1850-1855, 2008.

17 Ogura K, Yanagie H, Eriguchi M, Lehmann EH, Kuhne G, Bayon G and Kobayashi H: Neutron capture autoradiographic study of the biodistribution of ^{10}B in tumor-bearing mice. Appl Radiat Isot *61*: 585-590, 2004.

18 Arias H, Palacios D, Sajo-Bohus L and Viloria T: Alternative procedure for LR 115 chemical etching and alpha tracks counting. Radiat Meas *40*: 357-362, 2005.

19 Nikezic D and Yu KN: Profiles and parameters of tracks in the LR 115 detector irradiated with alpha particles. Nucl Instrum Methods Phys Res B *196*: 105-112, 2002.

20 Dwaikat N, Safarini G, El-hasan M and Iida T: CR-39 detector compared with Kodalpha film type (LR115) in terms of radon concentration. Nucl Instrum Meth A *574*: 289-291, 2007.

21 Coderre JA, Chanana AD, Joel DD, Elowitz EH, Micca PL, Nawrocky MM, Chadha M, Gebbers JO, Shady M, Peress NS and Slatkin DN: Biodistribution of boronophenylalanine in patients with glioblastomamultiforme: boron concentration correlates with tumor cellularity. Radiat Res *149*: 163-170, 1998.

22 Wang HE, Liao AH, Deng WP, Chang PF, Chen JC, Chen FD, Liu RS, Lee JS and Hwang JJ: Evaluation of 4-borono-2-^{18}F-fluoro-L-phenylalanine-fructose as a probe for boron neutron capture therapy in a glioma-bearing rat model. J Nucl Med *45*: 302-308, 2004.

23 Schipper ML, Cheng Z, Lee SW, Bentolila LA, Iyer G, Rao J, Chen X, Wu AM, Weiss S and Gambhir SS: MicroPET-based biodistribution of quantum dots in living mice. J Nucl Med *48*: 1511-1518, 2007.

24 Hsiao MC and Jiang SH: A characterization study of Gafchromic EBT film as a two-dimensional dosimeter. Nucl Technol *168*: 191-195, 2009.

25 Hsiao MC, Chen WL, Tsai PE, Huang CK, Liu YH, Liu HM and Jiang SH: A preliminary study on using the radiochromic film for 2D beam profile QC/QA at the THOR BNCT facility. Appl Radiat Isot *69*: 1915-1917, 2011.

26 Imahori Y, Ueda S, Ohmori Y, Sakae K, Kusuki T, Kobayashi T, Takagaki M, Ono K, Ido T and Fujii R: Positron emission tomography-based boron neutron capture therapy using boronophenylalanine for high-grade gliomas: Part I. Clin Cancer Res *4*: 1825-1832, 1998.

27 Takahashi Y, Imahori Y and Mineura K: Prognostic and therapeutic indicator of fluoroboronophenylalanine positron emission tomography in patients with gliomas. Clin Cancer Res *9*: 5888-5895, 2003.

28 Linko S, Revitzer H, Zilliacus R, Kortesniemi M, Kouri M and Savolainen S: Boron detection from blood samples by ICP-AES and ICP-MS during boron neutron capture therapy. Scand J Clin Lab Invest *68*: 696-702, 2008.

29 Laakso J, Kulvik M, Ruokonen I, Vahatalo J, Zilliacus R, Farkkila M and Kallio M: Atomic emission method for total boron in blood during neutron-capture therapy. Clin Chem *47*: 1796-1803, 2001.

30 Santa Cruz GA and Zamenhof RG: The microdosimetry of the B-10 reaction in boron neutron capture therapy: A new generalized theory. Cancer Res *162*: 702-710, 2004.

31 Coderre JA, Glass JD, Fairchild RG, Roy U, Cohen S and Fand I: Selective targeting of boronophenylalanine to melanoma in BALB/c mice for neutron capture therapy. Cancer Res *47*: 6377-6383, 1987.

32 Ono K, Masunaga SI, Kinashi Y, Takagaki M, Akaboshi M, Kobayashi T and Akuta K: Radiobiological evidence suggesting heterogeneous microdistribution of boron compounds in tumors: its relation to quiescent cell population and tumor cure in neutron capture therapy. Int J Radiat Oncol Biol Phys *34*: 1081-1086, 1996.

33 Yoshida F, Matsumura A, Shibata Y, Yamamoto T, Nakauchi H, Okumura M and Nose T: Cell cycle dependence of boron uptake from two boron compounds used for clinical neutron capture therapy. Cancer Lett *187*: 135-141, 2002.

Received May 26, 2012
Revised June 11, 2012
Accepted June 12, 2012